Virus Research 265 (2019) 132–137

Contents lists available at ScienceDirect

Virus Research

journal homepage: www.elsevier.com/locate/virusres

Short communication

Positive charge of Arg-201 on hemagglutinin is required for the binding of H6N1 avian influenza virus to its target through a two-step process

Ming-Shou Hsieh[a], Yuan-Chih Chang[b], Jie-Long He[c], Rong-Huay Juang[a,d,*]

[a] Institute of Biotechnology, National Taiwan University, Taipei, 10617, Taiwan
[b] Institute of Cellular and Organismic Biology, Academia Sinica, No. 128, Section 2 Academia Road, Nankang, Taipei, 115, Taiwan
[c] Department of Post-Baccalaureate Veterinary Medicine, Asia University, Taichung, 413, Taiwan
[d] Department of Biochemical Science and Technology, National Taiwan University, Taipei, 10617, Taiwan

ARTICLE INFO

Keywords:
Avian influenza virus
Charged amino acid
H6N1 subtype
Hemagglutinin
Receptor binding site
Two-step binding process

ABSTRACT

In our previous study, we produced a monoclonal antibody EB2 that recognized an epitope in the HA1 domain on the hemagglutinin (HA) of H6N1 influenza virus (A/chicken/Taiwan/2838 V/00). The residue Arg-201 (R201) on this epitope was protected by the glycan at Asn-167 (N167) from tryptic digestion; therefore, the infectivity of the virus was retained. R201 was extremely conserved in various subtypes of the influenza virus. To explore the role of R201 and the protecting glycan, we developed a bi-cistronic baculovirus expression system for the production of H6HA1 and H6HA0 (nearly full-length HA), which were glycosylated in insect cells. The expressed H6HA1 was mostly found in the trimeric form, and the H6HA0 protein was only found in the monomeric form. The trimeric H6HA1 was resistant to tryptic digestion; however, it could not bind to fetuin, a glycoprotein containing sialylated N-linked and O-linked glycans. By contrast, the monomeric H6HA0 could bind to fetuin but was sensitive to tryptic digestion. We found that the positive charge on R201 was critical for binding HA to the negatively charged surface of host cells because the mutant R201A of H6HA0 lost its binding capacity substantially. Moreover, this binding capacity was dependent on the pH value and inhibited by free electrically charged amino acids. We propose a two-step model for binding the influenza virus with a host cell. The first step involved the specific recognition of the receptor binding site on HA to the sialylated glycan on the host cell. After the virus is engulfed by the acidic endosome, R201 could bind to the cell surface with stronger interactions and trigger the fusion process.

1. Arg-201 on hemagglutinin of H6N1 influenza virus is protected by a glycan at Asn-167

In our previous study (He et al., 2014), we found a monoclonal antibody EB2 that recognized a short peptide (RYVRMGTESMN) on the head domain (HA1) of hemagglutinin (HA) from H6N1 influenza virus (A/chicken/Taiwan/2838 V/00). The second Arg on this peptide (Arg-201, R201) was extremely conserved among most subtypes of the influenza virus and was a dominant cleavage site for trypsin (Table 1). Nonetheless, this peptide was protected by a nearby glycan at Asn-167 (N167) and escaped the tryptic cleavage to retain viral infectivity (He et al., 2015). These experiments were conducted using purified virus particles from chicken eggs or recombinant HA1 fragment expressed in *E. coli* that was not glycosylated. Therefore, we developed a secretory bi-cistronic baculovirus expression system to produce HA1 protein in insect cells, which was secreted into the medium (Hsieh et al., 2018).

By utilizing this insect expression system, we produced the H6N1 HA1 protein (H6HA1) that was fully glycosylated because the molecular mass of H6HA1 decreased if it was treated with glycosidase (PNGase-F) to remove glycans (Suppl. Fig. 1A). The H6HA1 protein that was devoid of glycan became very sensitive to trypsin (Suppl. Fig. 1B). These results were consistent with our previous observations (He et al., 2015); however, an insect expression system was used in this study. We also expressed the H6HA0 protein that extended from the C-terminus of H6HA1 and nearly covered the full length of H6HA by using the chemical synthesis method. In accordance with our previous results (Hsieh et al., 2018), we found that an extensive part of the expressed H6HA1 protein was assembled in the trimeric form when observed on the SDS-PAGE blot (Fig. 1A). This H6HA1 trimeric form transformed to monomeric after denaturation by heating. However, H6HA0 was expressed as a monomer only, since the carboxyl- terminal trimerization domain was not included in our construct (Krammer et al., 2012). These

* Corresponding author. Present address: Graduate Institute of Applied Science and Technology, National Taiwan University of Science and Technology, Taipei, 10607, Taiwan.
E-mail address: juang@ntu.edu.tw (R.-H. Juang).

https://doi.org/10.1016/j.virusres.2019.03.018
Received 5 January 2019; Received in revised form 17 February 2019; Accepted 21 March 2019
Available online 26 March 2019
0168-1702/ © 2019 Elsevier B.V. All rights reserved.

Table 1
Comparison of the tryptic cleavage sites at R201, glycosylation sites at N167, and mAb EB2 epitopes on HA1 sequences of H6N1 viruses[a].

	Global		North America		Europe		Asia		China		Hong Kong		Taiwan	
	Number of matching	Percentage	Number of matching	Percentage	Number of matching	Percentage	Number of matching	Percentage	Number of matching	Percentage	Number of matching	Percentage	Number of matching	Percentage
Cleavage site R201 (K201)[b]	477/477	100%	228/228	100%	27/27	100%	212/212	100%	99/99	100%	29/29	100%	59/59	100%
Glycosylation site N167	434/477	90.9%	196/228	86.0%	25/27	92.5%	199/212	93.8%	96/99	96.9%	27/29	93.10%	57/59	96.6%
mAb EB2 epitope	453/477	94.9%	223/228	97.8%	25/27	92.5%	194/212	91.5%	97/99	97.9%	27/29	93.10%	46/59	77.9%

[a] We examined 477 HA1 sequences of H6N1 viruses obtained from GISAID (Global Initiative on Sharing Avian Influenza Data; http://platform.gisaid.org/).
[b] Among all 477 HA1 sequences, only two were found using K201 instead of R201 (0.4%).

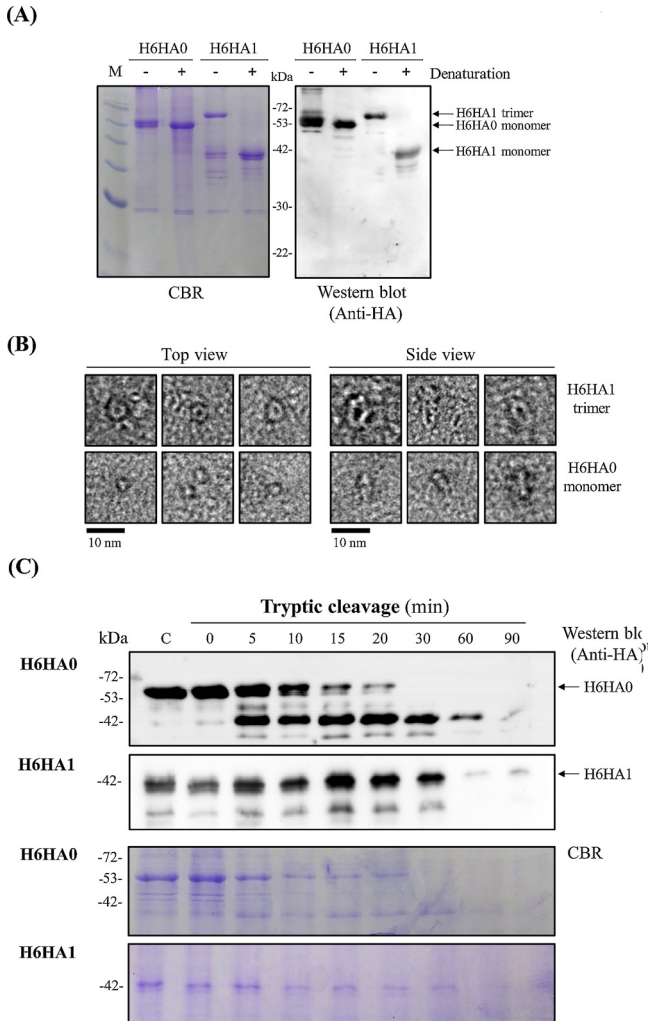

Fig. 1. H6HA proteins were expressed in insect cells and tested for proteolytic resistance.
H6HA0 or H6HA1 were produced in insect cells as described in our previous report (Hsieh et al., 2018). The H6HA0 used in this study contained 515 amino acids, followed by a His-tag in the C-terminus. This H6HA0 was prepared by extending the H6HA1 sequence (329 amino acids) to complete the C-terminal HA2 domain by using the chemical synthesis method. The gene fragment was synthesized and cloned by Mission Biotech, Taiwan. (A) H6HA1 was expressed mostly in the trimer, as observed on the SDS-PAGE blot. This trimeric form was transformed into monomeric if denatured by heating at 55 °C for 5 min in 10 mM dithiothreitol. However, H6HA0 only produced a monomer. (B) The expressed H6HA1 displayed its trimer structure when transmittance electron microscopy was conducted using the negative staining method (Fera et al., 2012). However, H6HA0 was only observed as a monomer. (C) The expressed proteins were treated with trypsin by following our previous protocol (He et al., 2015). H6HA1 exhibited better resistance to proteolysis than H6HA0. The molar ratios of H6HA1 or H6HA0 were adjusted to be equivalent by using an unequal amount of protein based on their molecular mass. In each tryptic digestion test, 26 μg of H6HA0 or 20 μg of H6HA1 was mixed with 0.1 μg of trypsin (anti-HA, anti-hemagglutinin mAb EB2; CBR, Coomassie Brilliant Blue R).

observations were further confirmed by transmission electron microscopy data (Fig. 1B). H6HA1 displayed a circular trimeric structure, and H6HA0 exhibited the monomeric form. Compared with H6HA1, the expressed H6HA0 presented lower resistance to tryptic digestion (Fig. 1C).

We generated several mutants of H6HA1 in which the glycosylation sites were selectively mutated (Fig. 2A). Mutant N167A replaced the Asn-167 site with Ala. Conversely, mutant M3 retained the Asn-167 site

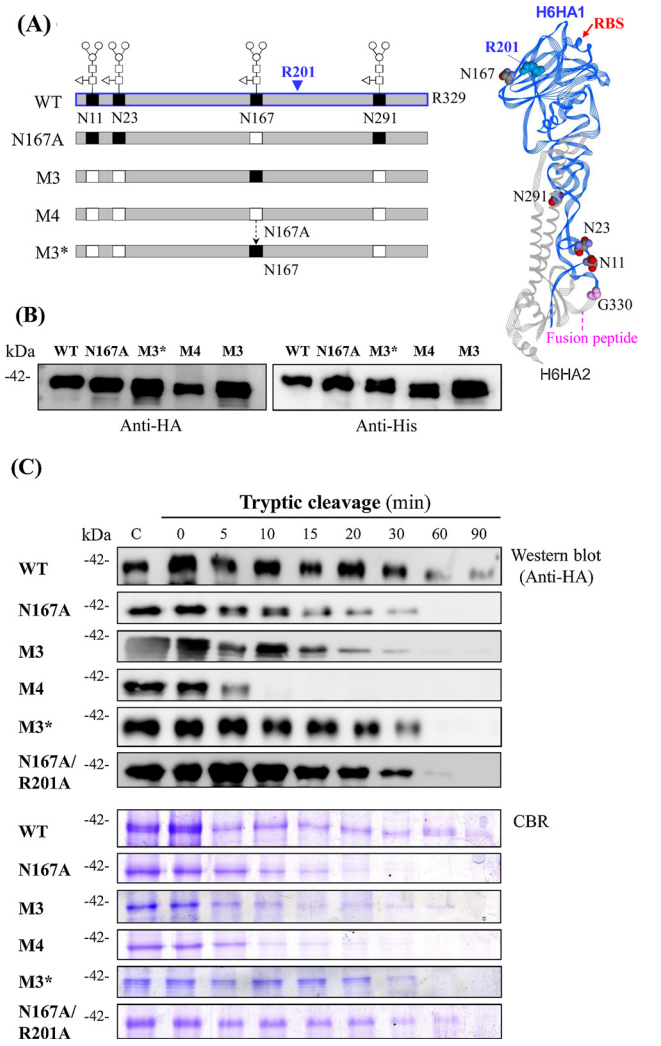

Fig. 2. Mutations at glycosylation sites on H6HA1 decreased the protection by a glycan against tryptic digestion.
(A) Several H6HA1 mutants were prepared by replacing Asn glycosylation sites with Ala based on the methods in our previous report (Hsieh et al., 2018). Mutant N167A replaced N167 with Ala. Mutant M3 replaced all glycosylation sites except the site at N167. Mutant M4 removed all the four glycans. The N167A on M4 was further reversed to N167 and produced the mutant M3*. The glycan trees on the wild-type of H6HA1 (WT) are schematic. The spatial locations of these glycosylation sites and R201 were labeled using a ribbon model on the right panel. The blue ribbon displays the HA1 domain of HA, and the gray ribbon is HA2. G330 is the Gly residue that leads the fusion peptide on HA2 after a tryptic cleavage at R329-G330. The RBS was indicated by an arrow. This model was prepared by Discovery Studio 2.5 (Accelrys, San Diego, CA), as described in our earlier report (He et al., 2015). (B) All mutants efficiently produced recombinant proteins when checked on Western blots. The molecular mass of the mutants decreased slightly because some glycans were removed. (C) The expressed proteins were treated with trypsin by following our previous protocol (He et al., 2015) and revealed diverse resistance to tryptic digestion. A mutant (N167A/R201A) with double mutation was also included for comparison (anti-His, anti-histidine tag).

but removed the remaining three sites (N11A, N23A, and N291A). Although all the glycosylation sites were replaced with Ala in mutant M4, we restored the mutation at N167A back to Asn-167 and produced the mutant M3*. Therefore, mutant M3* was equivalent to mutant M3 in the amino acid sequence. All these mutants efficiently produced recombinant proteins (Fig. 2B). The molecular mass of all mutants decreased as glycosylation sites were removed. Moreover, the mutants exhibited different levels of resistance to tryptic digestion (Fig. 2C). Compared with the wild-type, all mutants were sensitive to trypsin. However, M4 was extremely sensitive and disappeared within 10 min after treating with trypsin. N167A, M3, and M3* exhibited very similar degree of resistance and disappeared within 60 min. Notably, only one glycan was removed for mutant N167A; however, M3 and M3* lost three glycans. These results were consistent with our previous observations that N167 glycan might serve a critical role in protecting the R201 site on the head of HA (He et al., 2015). Moreover, we produced a mutant with double mutation (N167A/R201A), which exhibited slightly better resistance than the single mutation mutant N167A.

The expressed proteins of H6HA1 and its mutants were used to immunize mice. The titers of all mutants were considerably lower than the wild-type of H6HA1 (Suppl. Fig. 2). Evidently, M4 exhibited the lowest titer through the entire immunization process. The immune response of these antigens totally reflected their resistance against proteolysis in Fig. 2C. The low titer for mutants might be basically due to the degradation of antigens in the immunized animal.

2. Positive charge of Arg-201 might contribute to binding HA to the target

Among the four glycosylation sites, three glycans are located in the lower half of the HA, which might protect the trypsin cutting site at R329-G330 (Chen et al., 1998). The opening of this site generates a new N-terminal (G330) and releases the fusion peptide on HA2 (Fig. 2A, right panel) (Cross et al., 2009). Only the N167 glycan is located at the top of HA, and this glycan protects the nearby R201 from proteolysis (Fig. 2C). When we examined the corresponding amino acid sequences on HA from 477 H6N1 subtype, the R201 (or K201) site were 100% conserved (Table 1). Moreover, the analysis of HA from other subtypes also presented similar results (Suppl. Table 1 and Suppl. Fig. 3), thus implying that the positive charge at R201 serves a critical role.

One possible role of the positive charge at R201 was to facilitate the binding of a virus particle to the negatively charged surface on the host cell. Other studies also reported the influence of charged amino acids on the binding of HA with its targets (Soundararajan et al., 2009; Kobayashi and Suzuki, 2012). Based on this assumption, we measured the binding capacity of H6HA by coating fetuin on the enzyme-linked immunosorbent assay plate (ELISA plate), thus adding H6HA1 or H6HA0 to bind the immobilized fetuin. Then, anti-His antibody-enzyme conjugate was added to detect H6HA on the plate, and the absorbance at 450 nm was measured (Takemoto et al., 1996; Jiang and Eichelberger, 2015). In addition to the expressed wild-type proteins of H6HA1 and H6HA0, we constructed three mutants of H6HA0 at R201 by replacing Arg with Ala (R201A), Asp (R201D), or Lys (R201 K). Fig. 3A presents that the binding capacity of R201A, a mutant of H6HA0, reduced considerably. Moreover, a negatively charged substitution (R201D) totally eliminated the binding capacity. Interestingly, Lys substitution for Arg (R201 K) significantly enhanced the binding of H6HA0 to fetuin. Conversely, H6HA1 exhibited no capacity of binding to fetuin, which might be due to the lack of the HA2 domain (Rachakonda et al., 2007). Another possibility is that the quaternary structure of HA can influence the binding of H6HA1. To confirm the observations on ELISA, we examined the binding on a protein blot in which fetuin was immobilized by protein transfer after SDS-PAGE. Subsequently, H6HA or its mutants were added to bind the fetuin (Fig. 3B). Only the wild-type of H6HA0 or the R201 K mutant bound to the blot; no binding was observed for H6HA1, and the H6HA0 mutants (R201A or R201D). Consistently, R201 K presented a stronger band intensity on the blot than the wild-type.

Above observations suggest that the positive charge on R201 might serve a critical role in the binding of H6HA0 to fetuin. Moreover, the replacement of Arg with Lys on H6HA0 presented a stronger capacity of binding to fetuin. When we examined the sequences of H6HA, only a very small percentage of HA was observed using K201 (Table 1). There might be some evolutionary pressure to select Arg instead of Lys. To

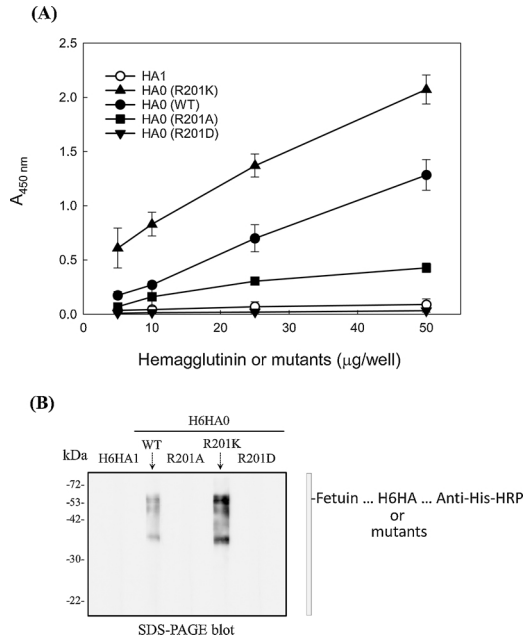

Fig. 3. H6HA0 and its R201 mutants exhibited varying capacities of binding to fetuin.

H6HA0 mutants at R201 (R210A, R210 K, and R201D) and the H6HA wild-types were expressed in insect cells and isolated for examining their capacity of binding to fetuin. (A) The expressed proteins were analyzed by using ELISA plates coated with fetuin (Jiang and Eichelberger, 2015). Contrary to the wild-type H6HA0 (WT, closed circle), the wild-type H6HA1 exhibited no capacity of binding to fetuin (open circle). Mutants of H6HA0 displayed varying influence on the binding capacity. R201D lost its binding capacity completely, but R201 K presented a stronger binding capacity than WT. (B) The binding of H6HA to fetuin was further confirmed by transferring fetuin onto a protein blot after SDS-PAGE. The blot was then incubated with H6HA or its mutants and was revealed using anti-His antibody conjugated with horse radish peroxidase (HRP). A schematic was presented on the right panel. Both ELISA and blot methods used the same procedure for binding and detection.

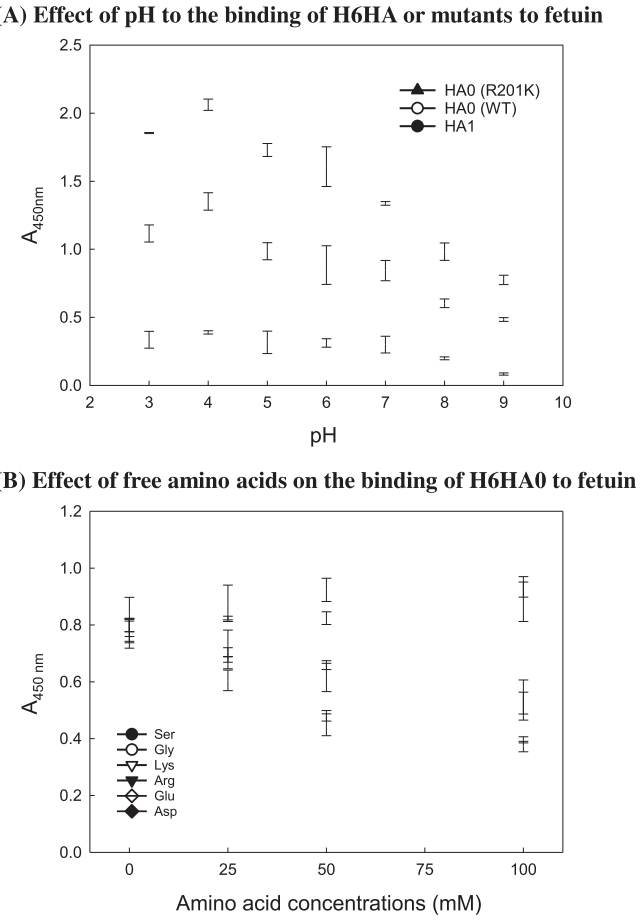

Fig. 4. The binding of H6HA0 to fetuin was affected by pH and electrostatically charged free amino acids.

(A) In acidic conditions, H6HA0 presented stronger binding to fetuin. (B) Some positively or negatively charged amino acids inhibited the binding of H6HA0 to fetuin.

achieve an accurate comparison between the Arg and Lys mutants in above experiments, we carefully estimated the amount of expressed proteins and used the optimal conditions for the immobilization of fetuin on the blots (Suppl. Fig. 4).

Subsequently, we determined that the binding of H6HA0 to fetuin was dependent on pH (Fig. 4A). An acidic environment of approximately pH 4 caused the binding capacity to be the maximum. The binding declined to approximately half at a neutral pH when observed on the ELISA plate. Apparently, a lower pH value caused the electric density at R201 to be more positively charged, thus resulting in a stronger binding. At a low pH (4.9), HA was in a conformation that can trigger the fusion of viral and host membranes (Böttcher et al., 1999; Huang et al., 2003; Di Lella et al., 2016). Therefore, a low pH favored both the binding of H6HA to the target and the following membrane-fusion step (Niles and Cohen, 1991; Skehel and Wiley, 2000; Di Lella et al., 2016). We further examined the effects of several free amino acids on the binding of H6HA0 to fetuin (Fig. 4B). Neutral amino acids revealed no effect on the binding (Gly & Ser); however, positively or negatively charged amino acids obviously interfered with the binding (Arg, Lys, Glu, and Asp). Interestingly, the acidic amino acids (Glu and Asp) exhibited stronger inhibition than the basic amino acids (Arg and Lys).

3. Two binding steps for the first encounter of influenza virus to its host

In this study, we expressed two groups of HA proteins in insect cells (Fig. 1). H6HA1 exhibited higher resistance against proteolysis than H6HA0, but lost its capacity of binding to fetuin. This trypsin resistance was because the glycan at N167 protected R201 (Fig. 2). Conversely, H6HA0 was sensitive to proteolysis (Fig. 1) but presented a stronger capacity of binding to fetuin, which might be due to the positive charge of R201 (Figs. 3 and 4). These diverse behaviors can be due to their quaternary protein structures because H6HA1 was mainly expressed in the trimeric form and H6HA0 was monomeric (Fig. 1). The steric structure of HA could influence both the resistance to proteolysis and the binding capacity, which originated from the spatial interaction between R201 and glycan at N167. We will address this point in our next report.

Clearly, the R201 residue on H6HA is critical for binding a virus to a host. However, the receptor binding site (RBS) constantly exists on the expressed HA molecules and the mutants. Then, a question concerning the role of RBS on the binding of HA to the host cell was posed. From the steric structure of HA (Fig. 2A), it was determined that both RBS and R201 are located on the head of HA. In the trimeric configuration, the three RBS sites are distributed around the outer edge of the head domain, thus leaving three R201 residues clumped in the center of the head (Fig. 5D). Our observations also suggested that the R201 cluster had stronger binding capacity than RBS because the R201A mutant completely lost its binding capacity under our experimental conditions (Fig. 3). These two binding sites may have different roles in binding a virus to its host cells. Chu and Whittaker (2004) noticed that influenza virus might bind its host and proceed internalization by a series of

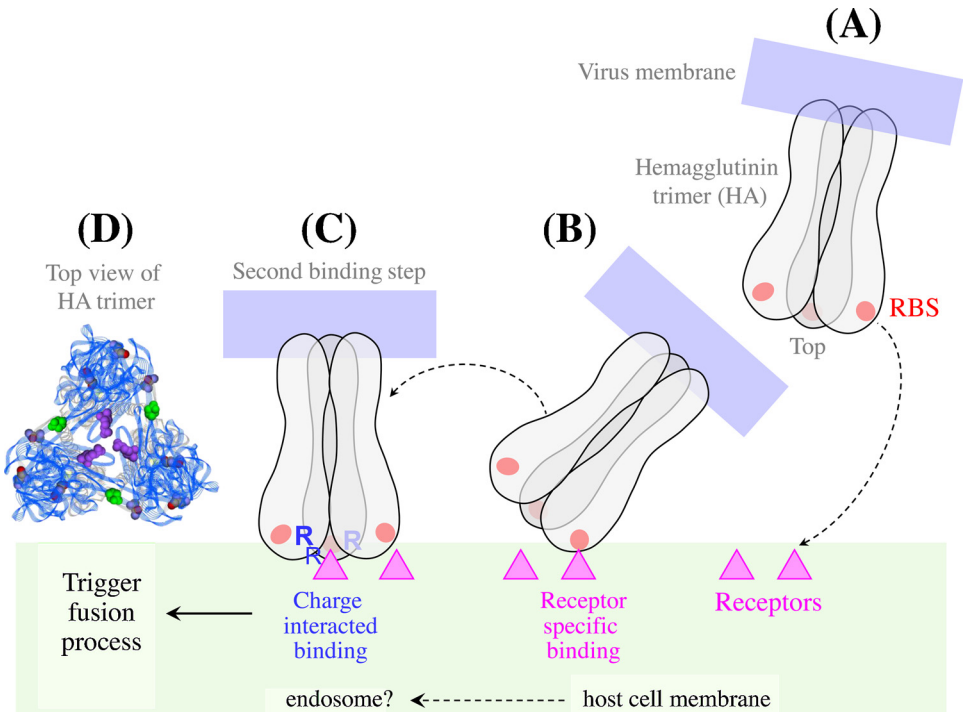

Fig. 5. Hypothetic model presented the two-step binding of HA to a host cell.
(A) HA on the virus particle approached the host cell. (B) HA specifically bound to the receptor on the host cell surface through RBS. The virus particle was engulfed into the host cell and then transported to an endosome. (C) The environment of the endosome was acidic. The R201 cluster on the top of the HA then bound to other host cell receptors through electrostatic interactions. (D) The positively charged Arg cluster (purple) was displayed in the top view of HA trimer. The second binding step might trigger the fusion process of virus invasion into the host cell.

distinct steps.

We postulate that there may be two steps during the encounter of the HA molecule to the target cell. Fig. 5 displayed this two-step binding model. First, RBS binds to the target in a specific mode, thus identifying the appropriate configuration of sialic acid linkage for a suitable host (Fig. 5A). After the specific recognition stage (Fig. 5B), the virus particle was engulfed into the host cell through endocytosis (Lakadamyali et al., 2004). In an acidic endosome environment, R201 was then induced to bind to the cell surface with stronger interactions (Fig. 5C), which are mainly due to the electrostatic interactions of three R201 residues against the negative charges on the host cell surface (Fig. 5D). The second step guides the HA trimer to sit in an upright position to obtain a correct angle to proceed to the following invasion step (Fig. 5C). This step may trigger the activation of a fusion peptide to insert it into the host membrane (Carr and Kim, 1994; Yu et al., 1994). This two-step binding model may lead to a new strategy for blocking the binding of influenza virus to the host cell and preventing the invasion of the virus.

Declaration of conflicting interests

The authors declare no conflict of interest.

Funding source

This work was supported by the Ministry of Science and Technology, Taiwan, ROC (grant numbers: 103-2321-B-002-060 and 104-2321-B-002-018).

Acknowledgements

We thank GGA Corporation, Molecular Science Center (Taiwan) for constructing the molecular model of 2838 HA trimer, and Dr. Wang Chuen Kai and Mr. Huang Xiu-Xuan of New Century Biotech Co., Ltd. for the 3D printing of HA models.

Appendix A. Supplementary data

Supplementary material related to this article can be found, in the online version, at doi:https://doi.org/10.1016/j.virusres.2019.03.018.

References

Böttcher, C., Ludwig, K., Herrmann, A., van Heel, M., Stark, H., 1999. Structure of influenza haemagglutinin at neutral and at fusogenic pH by electron cryo-microscopy. FEBS Lett. 463, 255–259.
Carr, C.M., Kim, P.S., 1994. Flu virus invasion: halfway there. Science 266, 234–236.
Chen, J., Lee, K.H., Steinhauer, D.A., Stevens, D.J., Skehel, J.J., Wiley, D.C., 1998. Structure of the hemagglutinin precursor cleavage site, a determinant of influenza pathogenicity and the origin of the labile conformation. Cell 95, 409–417.
Chu, V.C., Whittaker, G.R., 2004. Influenza virus entry and infection require host cell N-linked glycoprotein. Proc. Natl. Acad. Sci. U. S. A. 101, 18153–18158.
Cross, K.J., Langley, W.A., Russell, R.J., Skehel, J.J., Steinhauer, D.A., 2009. Composition and functions of the influenza fusion peptide. Protein Pept. Lett. 16, 766–778.
Di Lella, S., Herrmann, A., Mair, C.M., 2016. Modulation of the pH stability of influenza virus hemagglutinin: a host cell adaptation strategy. Biophys. J. 110, 2293–2301.
Fera, A., Farrington, J.E., Zimmerberg, J., Reese, T.S., 2012. A negative stain for electron microscopic tomography. Microsc. Microanal. 18, 331–335.
He, J.L., Hsieh, M.S., Juang, R.H., Wang, C.H., 2014. A monoclonal antibody recognizes a highly conserved neutralizing epitope on hemagglutinin of H6N1 avian influenza virus. Vet. Microbiol. 174, 333–341.
He, J.L., Chiu, Y.C., Chang, S.C., Wang, C.H., Juang, R.H., 2015. Glycosylation at hemagglutinin Asn-167 protects the H6N1 avian influenza virus from tryptic cleavage at Arg-201 and maintains the viral infectivity. Virus Res. 197, 101–107.
Hsieh, M.S., He, J.L., Wu, T.Y., Juang, R.H., 2018. A secretory bi-cistronic baculovirus expression system with improved production of the HA1 protein of H6 influenza virus in insect cells and *Spodoptera litura* larvae. J. Immunol. Methods 459, 81–89.
Huang, Q., Sivaramakrishna, R.P., Ludwig, K., Korte, T., Bottcher, C., Herrmann, A., 2003. Early steps of the conformational change of influenza virus hemagglutinin to a fusion active state: stability and energetics of the hemagglutinin. Biochim. Biophys. Acta 1614, 3–13.
Jiang, L., Eichelberger, M.C., 2015. Evaluation of Epic label-free technology to quantify functional recombinant hemagglutinin. Biol. Proced. Online 17, 7.
Kobayashi, Y., Suzuki, Y., 2012. Compensatory evolution of net-charge in influenza a virus hemagglutinin. PLoS One 7, e40422.
Krammer, F., Margine, I., Tan, G.S., Pica, N., Krause, J.C., Palese, P., 2012. A carboxy-terminal trimerization domain stabilizes conformational epitopes on the stalk domain of soluble recombinant hemagglutinin substrates. PLoS One 7, e43603.
Lakadamyali, M., Rust, M.J., Zhuang, X., 2004. Endocytosis of influenza viruses. Microbes Infect. 6, 929–936.
Niles, W.D., Cohen, F.S., 1991. The role of N-acetylneuraminic (sialic) acid in the pH dependence of influenza virion fusion with planar phospholipid membranes. J. Gen. Physiol. 97, 1121–1140.
Rachakonda, P.S., Veit, M., Korte, T., Ludwig, K., Bottcher, C., Huang, Q., Schmidt, M.F.,

Herrmann, A., 2007. The relevance of salt bridges for the stability of the influenza virus hemagglutinin. FASEB J. 21, 995–1002.
Skehel, J.J., Wiley, D.C., 2000. Receptor binding and membrane fusion in virus entry: the influenza hemagglutinin. Annu. Rev. Biochem. 69, 531–569.
Soundararajan, V., Tharakaraman, K., Raman, R., Raguram, S., Shriver, Z., Sasisekharan, V., Sasisekharan, R., 2009. Extrapolating from sequence–the 2009 H1N1' swine' influenza virus. Nat. Biotechnol. 27, 510–513.
Takemoto, D.K., Skehel, J.J., Wiley, D.C., 1996. A surface plasmon resonance assay for the binding of influenza virus hemagglutinin to its sialic acid receptor. Virology 217, 452–458.
Yu, Y.G., King, D.S., Shin, Y.K., 1994. Insertion of a coiled-coil peptide from influenza virus hemagglutinin into membranes. Science 266, 274–276.